Validity of the coupled-channel reduction in three-body scattering

O. A. Rubtsova, V. I. Kukulin, and V. N. Pomerantsev
Institute of Nuclear Physics, Moscow State University, 119991 Moscow, Russia
(Received 17 August 2011; published 24 October 2011)

Near-threshold singularities of elastic scattering amplitudes in the coupled-channel reduction for collisions of weakly bound projectiles with nuclear targets are studied within the framework of the three-body scattering problem. The initial three-body scattering amplitudes are demonstrated to have artificial nonphysical singularities near the pseudo-thresholds of inelastic channels. These singularities, similar to the atomic physics applications, are originated from the discretization of the projectile sub-Hamiltonian continuum. However, in nuclear physics applications, the presence of imaginary parts in optical potentials for the projectile fragments and target suppresses strongly all the irregularities. The complete wave-packet discretization of three-body continuum is shown to lead to quite smooth approximations for elastic partial amplitudes as functions of the total energy. Simultaneously we prove that the pseudostate-continuum approximation for the channel three-body resolvent is rather accurate when solving the three-body scattering problems.

DOI: 10.1103/PhysRevC.84.044002 PACS number(s): 24.10.Eq, 03.65.Nk, 21.45.−v, 25.45.De

I. MOTIVATION OF THE STUDY

One of the most popular methods for solving quantum scattering problems of composite particles in atomic, molecular and nuclear physics is a reduction to the coupled-channel scheme. In fact, the majority of practical applications toward the solution of realistic scattering problems is based just on such a coupled-channel approximation (CCA) [1–11]. Despite some special details, such approaches have common features related to employment of some specific finite L_2 basis for the representation of the excitations of the projectile (or target) into continuum states. In this way, the continuous spectrum of the projectile and/or target becomes discretized. The effects of such L_2 continuum discretization to the energy behavior of elastic scattering amplitudes have been studied in detail previously within the pseudo-state expansion and strong-coupling CCA methods mainly in the atomic physics applications [1,2]. These effects are related to the appearance of false resonances in three-body spectra near discrete pseudostate eigenenergies and, as a sequence, they lead to a rather singular energy behavior of elastic amplitudes. In nuclear physics, this CCA approach is often done in the form of the so-called continuum-discretized coupled-channel (CDCC) method, which is quite popular for the treatment of composite particle scattering by nuclear target [3–7]. The approach can also be considered as a variant of the general CCA scheme. Thus, quite similar to other continuum discretization schemes, one should also observe, in general, some energy singularities due to false thresholds corresponding to pseudostate energies.

In previous years, some active general discussions (see, e.g., Ref. [12]) have been dedicated to the validity of the CCA approaches in few-body scattering problems. One of the main difficulties in the rigorous substantiation of the CCA treatment for two- and few-body continuum states, like the CDCC approach, lies in the fact that some part of channels (usually the rearrangement channels) are neglected in such a treatment. So that one cannot compare, e.g., the CDCC solution in the case of three-body scattering with full Faddeev solution where the rearrangement channels are fully incorporated. On the other hand, the respective three-body Lippmann-Schwinger equation (taken in one channel) has a non-Fredholm kernel, so its direct numerical solution may lead to serious practical problems, e.g., divergences or nonphysical near-threshold singularities of the scattering amplitudes. However, as far as the present authors are aware, the effects of such nonphysical energy singularities to the scattering observables within the conventional coupled-channel reduction have, to date, not been studied in nuclear physics (e.g., in the CDCC-approach).

Thus, two important problems are related to the general coupled-channel reduction for few- and many-body scattering problems. First, the convergence of the CCA solutions to the exact ones with increasing the number of channels involved. The second one is how to treat (or remove) the false energy singularities near the pseudo-thresholds and what is the real impact of these singularities in the calculated cross sections.

The present work is aimed to elucidate these two important issues and to shed some light on the validity of CCA in nuclear physics applications. Also, we study the character of the energy singularities and their dependence on the interactions involved in the couple-channel reduction in some test three-body scattering problems. So, as a first step we study the convergence of the CCA results to the exact ones and also the near-threshold singularities of the elastic scattering amplitude within the conventional Schroedinger CCA formalism. Then we present a new approach based on the wave-packet expansion basis [13–16] that makes it possible to smooth noticeably the artificial near-threshold singularities in many cases and get some regular (in energy) scattering amplitudes around the threshold energies.

Thus, we use the original wave-packet continuum discretization (WPCD) approach developed recently by the present authors [13–16]. This approach allows us to find an accurate solution of the initial three-body scattering problem for its consequent comparison to the CCA results. For this purpose we employ an integral formulation of the quantum scattering problem, which allows us to take into account different types of boundary conditions in the three-body

scattering [15]. So, the above discrete wave-packet approach allows us to compare directly the results of the CCA and the full three-body calculation within *the same* three-body model (i.e., *in the same model space*).

In our previous paper [13], we have found an excellent agreement between the results of our WPCD matrix approach and the conventional CDCC-method predictions at a few separate energies, i.e., without studying energy dependencies of the observables in a near-threshold region. In the present paper we have made a detailed and comprehensive comparison between the CCA and accurate results and we have studied the CCA impact on the energy behavior of the elastic scattering amplitudes in three-body scattering.

The structure of the paper is as follows. In the Sec. II we briefly outline the evaluation of the elastic scattering amplitude using the conventional Schröedinger and Lippmann–Schwinger CCAs. Section III is devoted to the description of the discretization scheme for the three-body Lippmann-Schwinger equation and the CCA method via wave-packet approach. The study of validity for the above general approaches for some test examples is presented in Sec. IV, while the WPCD results for the deuteron off ^{16}O target elastic scattering is discussed in the Sec. V. Our general conclusions are given in the Sec. VI.

II. COUPLED-CHANNEL REDUCTION IN THE THREE-BODY SCATTERING

A. Schröedinger equation formalism

We will consider the three-body Hamiltonian, which describes the scattering of the two-fragment composite projectile $\{12\}$ (deuteron or other light nucleus) off the structureless target A in the form

$$H = h_{12} + h_0 + V_{1A} + V_{2A}, \tag{1}$$

where h_{12} is the sub-Hamiltonian for the $\{12\}$-subsystem, the h_0 is the kinetic energy operator for the projectile center of mass. The optical potentials V_{1A} and V_{2A} of fragment-target interactions are usually assumed to be complex and energy-dependent. However, the smooth energy dependence of the input optical potentials is of no importance for our purposes in the study and, thus, we omit it here. Also, we assume that there is only one s-wave bound state $|z_0\rangle$ (say, a deuteron) with energy ϵ_0^* in the subsystem $\{12\}$, and also the spin-dependent effects as well as the Coulomb interaction will be ignored for simplicity.

The total wave-function of the system with the Hamiltonian Eq. (1) can be found from the three-body Schroedinger equation:

$$H|\Psi\rangle = E|\Psi\rangle, \tag{2}$$

where E is the total energy. Due to complex parts of the input optical potentials, there are no real bound states in the subsystems $\{1A\}$ and $\{2A\}$, so that the rearrangement channels can be neglected as well [3,12].

In the CCA approach, the total scattering wave function for the Hamiltonian Eq. (1) is expanded in some L_2-basis $\{|z_i\rangle\}_{i=0}^{N_{\rm eff}-1}$ corresponding to the projectile sub-Hamiltonian h_{12} eigenfunctions and eigenvalues in the sense that

$$\langle z_i|h_{12}|z_j\rangle = \delta_{ij}\epsilon_i^*, \tag{3}$$

where ϵ_i^* are the corresponding energies of the bound state and pseudostates of the system (so, the total basis dimension is $N_{\rm eff}$). Such a basis can be constructed, e.g., from the functions obtained via the diagonalization of h_{12} in some L_2-basis or from the stationary wave packet set accomplished with the bound-state wave function (see below). In the conventional approach, one uses the expansion of scattering wave functions in the basis set $\{z_i(\mathbf{r})\}$ in the coordinate representation

$$\Psi(\mathbf{r},\mathbf{R}) = \sum_{i=0}^{N_{\rm eff}-1} z_i(\mathbf{r})\chi_i(\mathbf{R}), \tag{4}$$

where $\mathbf{r}$ is the inner coordinate of the projectile, and $\mathbf{R}$ is the coordinate of its center of mass motion relative to the target. In the Eq. (4), the expansion coefficients $\chi_i(\mathbf{R})$ have the meaning of the relative motion wave function. These functions satisfy the system of the coupled-channel equations, which (after partial-wave expansion) takes the form:

$$\left[\frac{\hbar^2}{2m}\left(\frac{d^2}{dR^2} - \frac{L_i(L_i+1)}{R^2}\right) + (E-\epsilon_i^*)\right]\chi_i(R) = \sum_k W_{ik}(R)\chi_k(R), \quad i = 0,\ldots,N_{\rm eff}-1, \tag{5}$$

where m is the projectile-target reduced mass, L_i is the orbital angular momentum of the projectile-target relative motion in the channel i, and $W_{ik}(R)$ are the coupling potentials:

$$W_{ik}(R) = \langle z_i|V_{1A}\left(\left|\mathbf{R}+\tfrac{1}{2}\mathbf{r}\right|\right) + V_{2A}\left(\left|\mathbf{R}-\tfrac{1}{2}\mathbf{r}\right|\right)|z_k\rangle. \tag{6}$$

The boundary conditions at $R\to\infty$ for functions $\chi_i(R)$ corresponding to the scattering problem have a standard form: incoming and outgoing waves in open channels ($E-\epsilon_i^* > 0$) and decaying solutions in closed channels ($E-\epsilon_i^* < 0$):

$$\chi_i(R) \to h_L^{(-)}(P_0R)\delta_{i0} - \sqrt{\frac{P_i}{P_0}}h_L^{(+)}(P_iR)S_{i0}, \tag{7}$$

where $P_i = \sqrt{2m(E-\epsilon_i^*)}$, $h_L^{(\pm)}(x)$ are the spherical Riccati-Hankel functions, and $\{S_{i0}\}$ are the S-matrix elements. Here we assume that there is the incoming wave only in the channel 0. The S-matrix dimension is equal to the number of the open channels (the remaining elements of matrix S in Eq. (7) do not have direct physical meaning).

By solving Eq. (5) with a regular boundary condition at the origin $\chi_i(0) = 0$ and matching the numerical solutions with the asymptotical ones [Eq. (7)] at $R = R_0$ (R_0 is the boundary of the interaction region), one gets, eventually, the total multichannel S matrix.

The treatment of the closed channels represents in general a nontrivial numerical problem within the CCA approach. In the case of closed channels, there are the exponentially growing solutions along with the decaying (physical) ones, which lead to some instabilities and inaccuracies in the numerical solution of the CCA Eq. (5). To avoid such problems, we employed here the propagation matrix method [11]. The technique is based on the following observation: when matching the numerical

and asymptotical solutions at $R = R_0$, it is sufficient to know only the ratio of scattering wave functions at the neighboring points $D(R_0) = \chi(R_0)/\chi(R_0 + h)$ (where h is the integration step) while the wave functions $\chi_i(R)$ themselves are not required. So, instead of finding the scattering wave functions, one calculates a matrix containing such the ratios at all the integration mesh points and derives the total S-matrix from these [11]. This matrix of the ratios (it is called as a propagation matrix) is bounded except for a finite number of points. In the present work, we have used the above propagation matrix method [11] for practical solving of the differential CCA equations.

B. Integral equation formulation

In the case to be discussed, when the rearrangement channels can be neglected, the transition operator T which describes the elastic scattering of the projectile by the target nucleus as well as the projectile breakup is found from a single Lippmann-Schwinger equation (LSE) [13]:

$$T(E) = \bar{V} + \bar{V} G_{12}(E) T(E), \tag{8}$$

where $\bar{V} \equiv V_{1A} + V_{2A}$ is the so called external interaction and $G_{12} = [E + i0 - h_0 - h_{12}]^{-1}$ is the channel resolvent that determines the asymptotic states in the channel. This operator can be found as a convolution of the respective two-body subresolvents $g_{12}(\epsilon) = [\epsilon + i0 - h_{12}]^{-1}$ and $g_0(\varepsilon) = [\varepsilon + i0 - h_0]^{-1}$, i.e.,

$$G_{12}(E) = \frac{1}{2\pi i} \int_{-\infty}^{\infty} g_{12}(\epsilon) g_0(E - \epsilon)\, d\epsilon. \tag{9}$$

Further, we will employ spectral representations for the both resolvents, g_{12} and g_0, using complete sets of the eigenfunctions $|\psi_{12}(\epsilon)\rangle$ and $|\psi_0(\varepsilon)\rangle$ of the sub-Hamiltonians h_{12} and h_0, respectively. By substituting these spectral expansions into the convolution Eq. (9), one can get [13] two terms in three-body channel resolvent $G_{12}(E) = G_{12}^{BC}(E) + G_{12}^{2C}(E)$, where

$$\begin{aligned} G_{12}^{BC}(E) &= \int_0^{\infty} d\varepsilon \frac{|z_0, \psi_0(\varepsilon)\rangle\langle z_0, \psi_0(\varepsilon)|}{E + i0 - \epsilon_0^* - \varepsilon} \\ G_{12}^{2C}(E) &= \int_0^{\infty} d\epsilon \int_0^{\infty} d\varepsilon \frac{|\psi_{12}(\epsilon), \psi_0(\varepsilon)\rangle\langle\psi_{12}(\epsilon), \psi_0(\varepsilon)|}{E + i0 - \epsilon - \varepsilon}. \end{aligned} \tag{10}$$

Here the term $G_{12}^{BC}(E)$ corresponds to the bound-continuum (BC) couplings while the second term, $G_{12}^{2C}(E)$, corresponds to the continuum-continuum (2C) couplings of two subsystem spectra.

It is straightforward to show further, if one employs a pole approximation for the resolvent g_{12} for the discretized continuum in Eq. (9), viz.

$$g_{12}(\epsilon) \approx \sum_{i=0}^{N_{\rm eff}-1} \frac{|z_i\rangle\langle z_i|}{\epsilon - \epsilon_i^*}, \tag{11}$$

where $|z_i\rangle$ and ϵ_i^* are eigenstates and eigenenergies of the sub-Hamiltonian matrix h_{12} in two-body basis Eq. (3) (including the bound state energy ϵ_0^*), then the above three-body LSE Eq. (8) can be reduced to the multichannel two-body equations. As a result of the pole approximation Eq. (11), one gets the following representation for the three-body channel resolvent G_{12} [instead of the Eq. (10)]:

$$G_{12}(E) \approx \sum_{i=0}^{N_{\rm eff}-1} \int_0^{\infty} \frac{|z_i, \psi_0(\varepsilon)\rangle\langle z_i, \psi_0(\varepsilon)|}{E + i0 - \epsilon_i^* - \varepsilon} d\varepsilon, \tag{12}$$

where each term in the sum takes the form of the BC-part of the resolvent. One can refer to such an approximation as the Pseudostate-Continuum (PC) coupling.

After substitution of the representation Eq. (12) into three-body LSE Eq. (8), one gets the set of two-body coupled integral equations:

$$\begin{aligned} |\chi_i(E)\rangle &= |\psi_0(E - \epsilon_0^*)\rangle \delta_{i0} + \sum_k g_0(E - \epsilon_i^*) W_{ik} |\chi_k(E)\rangle, \\ & i = 0, \ldots, N_{\rm eff} - 1, \end{aligned} \tag{13}$$

where the coupling potentials W_{ik} are defined by Eq. (6). Equation (13) is equivalent to the differential system Eq. (5) with boundary condition Eq. (7).

III. THREE-BODY LIPPMANN-SCHWINGER EQUATION IN A DISCRETE REPRESENTATION

The initial three-body LSE Eq. (8) can be solved in the WPCD approach by using a discretization of continuous spectra of the both sub-Hamiltonians h_{12} and h_0. In this method, each spectrum is divided into nonoverlapping energy bins $[\epsilon_{i-1}, \epsilon_i]_{i=1}^{N_{\rm eff}-1}$ and $[\varepsilon_{j-1}, \varepsilon_j]_{j=1}^{M}$ with widths $D_i = \epsilon_i - \epsilon_{i-1}$ and $\Delta_j = \varepsilon_j - \varepsilon_{j-1}$, respectively. Then, one constructs stationary wave-packets in each bin in a standard way [17]:

$$|z_i\rangle = \frac{1}{\sqrt{D_i}} \int_{\epsilon_{i-1}}^{\epsilon_i} d\epsilon |\psi_{12}(\epsilon)\rangle, \tag{14}$$

$$|x_j\rangle = \frac{1}{\sqrt{\Delta_j}} \int_{\varepsilon_{j-1}}^{\varepsilon_j} d\varepsilon |\psi_0(\varepsilon)\rangle. \tag{15}$$

So, one uses the wave-packet states [Eq. (14)] jointly with the bound state function $|z_0\rangle$ as the basis set [Eq. (3)] in the {12}-subsystem and free wave-packet states [Eq. (15)] as basis states in the projectile-target subsystem.

Then, the three-body wave-packet (3WP) basis states corresponding to the discretization of the three-body continuum are built as products of two-body wave-packet basis states $|S_{ij}\rangle = |z_i, x_j\rangle$. From these orthonormalized basis states, one can construct a three-body projection operator:

$$\mathbb{P} = \sum_{i=0}^{N_{\rm eff}-1} \sum_{j=1}^{M} |z_i, x_j\rangle\langle z_i, x_j|.$$

Thus, after projection of the three-body wavefunctions and scattering operators, one gets the respective vectors and matrices in the 3WP space. Such a wave-packet representation is very convenient in various applications because it is *the eigen representation* for the projected channel Hamiltonian $H_{12} = h_{12} \oplus h_0$ and the basis states correspond to exact asymptotic states of the system.

In particular, the initial state wave function of the system $|\Psi_0(E)\rangle \equiv |z_0, \psi(E - \epsilon_0^*)\rangle$, which defines the asymptotic free

motion of the projectile, corresponds to a single basis state, i.e.,

$$\mathbb{P}|z_0, \psi_0(E-\epsilon_0^*)\rangle = \frac{|z_0, x_{j_0}\rangle}{\sqrt{\Delta_{j_0}}}, \quad (E-\epsilon_0^*) \in [\varepsilon_{j_0-1}, \varepsilon_{j_0}]. \tag{16}$$

One of the main advantages of the WPCD approach is the fact that the three-body channel resolvent operator $G_{12}(E)$ can be represented in the above wave-packet basis as *a diagonal matrix* [13–15]. So, when one applies such a wave-packet projection, one gets the following finite-dimensional representation for the three-body resolvent operator $\mathbb{G}_{12}(E) \equiv \mathbb{P}G_{12}(E)\mathbb{P}$:

$$\mathbb{G}_{12}(E) = \sum_{j=1}^{M} |z_0, x_j\rangle g_j(E-\epsilon_0^*)\langle z_0, x_j| + \sum_{i=1}^{N_{\rm eff}-1}\sum_{j=1}^{M} |z_i, x_j\rangle g_{ij}(E)\langle z_i, x_j|. \tag{17}$$

The first term is the discrete analog of the BC part of the channel resolvent while the second term is the discrete analog of the 2C-part of the operator [Eq. (10)]. Therefore, matrix elements g_j in the first and g_{ij} the second terms can be treated as eigenvalues of the channel resolvent matrix in the 3WP basis:

$$g_j(E-\epsilon_0^*) = \frac{1}{\Delta_j}\int_{\varepsilon_{j-1}}^{\varepsilon_j} \frac{d\varepsilon}{E+i0-\epsilon_0^*-\varepsilon}, \tag{17a}$$

$$g_{ij}(E) = \frac{1}{D_i\Delta_j}\int_{\epsilon_{i-1}}^{\epsilon_i}\int_{\varepsilon_{j-1}}^{\varepsilon_j} \frac{d\epsilon d\varepsilon}{E+i0-\epsilon-\varepsilon}. \tag{17b}$$

These eigenvalues only depend upon the partitions of the spectra of the two-body sub-Hamiltonians and can be found easily in an explicit form [16].[1]

Eventually, after the wave-packet projecting of the operators, all the terms in the three-body LSE take a matrix form and the T matrix can be found easily from a single matrix equation:

$$\mathbf{T} = \mathbf{V} + \mathbf{V}\mathbf{G}_{12}\mathbf{T}, \tag{18}$$

where $\mathbf{V}$ is the external interaction matrix in the three-body wave-packet basis, $\mathbf{G}_{12}$ is the diagonal matrix of the channel resolvent at the total energy E. To find the on-shell and half-shell T-matrix elements, it is sufficient to find the solution of Eq. (18) only for one column $t_p \equiv T_{p,p_0}, \quad p = 1, \ldots, \mathcal{N}$ [we use here the multi-index $p = (i, j)$, so that the label $p_0 = (0, j_0)$ corresponds to the initial state]. The respective solution can be found from the equation

$$(\mathbf{I} - \mathbf{V}\mathbf{G}_{12})t = v. \tag{19}$$

Here the notation is: $v_p \equiv V_{p,p_0}$, $p = 1, \ldots, \mathcal{N}$, and $\mathbf{I}$ is the unit matrix. The S-matrix elements are interrelated to the t-vector elements by the relationship

$$S_{\rm el}(E) = 1 - 2\pi i\frac{t_{p_0}}{\Delta_{j_0}}, \quad (E-\epsilon_0^*) \in [\varepsilon_{j_0-1}, \varepsilon_{j_0}]. \tag{20}$$

In the case of the CCA reduction (i.e., for the PC approximation in the WPCD), instead of Eq. (17), one gets the following finite-dimensional operator:

$$\mathbb{G}_{12}^{PC}(E) = \sum_{i=0}^{N_{\rm eff}-1}\sum_{j=1}^{M} |z_i, x_j\rangle g_j(E-\epsilon_i^*)\langle z_i, x_j|, \tag{21}$$

where all the eigenvalues of the channel resolvent in this case take the form of the BC-part eigenvalues[2] given in Eq. 17(a). So, the PC approximation corresponds to the case, when all the discretized states "loose" their widths. In such a PC approximation, the 3WP LSE Eq. (18) reduces to purely two-body equations for coupled channels, those are being discrete analogs of integral Eq. (13).

In this way, by making use the finite-dimensional representation given by Eq. (21) for the resolvent matrix in Eq. (19) and via solving the resulted matrix CCA equations, one can directly compare the full and CCA results for the initial three-body scattering problem.

IV. COMPARISON OF THE CCA AND FULL THREE-BODY CALCULATION RESULTS

To study a validity of the CCA reduction both in differential and integral equation formulations, we employ, at first, the test model with all the interactions given in the simple Gaussian form for two types of the projectile fragment-target interactions: (I) the case of weak and real fragment-target interaction potentials, when bound states in $\{1A\}$ and $\{2A\}$ subsystems are absent; (II) the case of complex fragment-target potentials when the real part of the $\{1(2)A\}$ potential gives one bound state in $\{1(2)A\}$ subsystem.

Below, three methods for calculation of scattering three-body observables will be applied: numerical solution of the CCA *differential equations* based on the propagation matrix method [11] (which we refer to as the differential CCA-calculation), solution of the LSE equation with PC approximation, which corresponds to the solution of the Eq. (13), and finally, full solution of the three-body LSE *without* the coupled-channel approximations. For the last two calculations, we will employ the WPCD method and will refer to the results as "integral CCA" and "full WP" results correspondingly. In this section, we discuss the dependence of the elastic scattering observables on the projectile kinetic energy $E_{\rm kin} \equiv E - \epsilon_0^*$, where ϵ_0^* is the projectile binding energy (negative).

[1] To avoid some possible additional irregularities near bin endpoints in such finite-dimensional approximations for the channel resolvent, we usually add the averaging procedure for the eigenvalues Eq. (17) over the external total energy (see the details in Ref. [14]).

[2] In practical calculations, one should also use here additional averaging over external total energy E.

A. The model and the basis parameters

The interaction between fragments 1 and 2 in the projectile is taken in the form of a Gaussian potential:

$$V_{12}(r) = V_0 \exp(-\gamma r^2), \tag{22}$$

with parameters $V_0 = -72.15$ MeV, $\gamma = 0.454$ fm^{-2}. The particles 1 and 2 are assumed to be the same and their masses are equal to 1 a.m.u.

The interaction potentials in $\{1(2)A\}$ subsystems are taken also in the Gaussian form

$$V_{iA}(r_i) = U_0 \exp\left(-\beta r_i^2\right), \quad i = 1, 2, \tag{23}$$

where the potential parameters for the models are the following:

$$\text{I}: \quad U_0 = -15.0\ \text{MeV}, \quad \beta = 0.444\ \text{fm}^{-2}, \tag{23a}$$

$$\text{II}: \quad U_0 = -50.0(1 + i \cdot q)\ \text{MeV}, \quad \beta = 0.444\ \text{fm}^{-2}, \tag{23b}$$

and we will vary the imaginary parts of the potential depth U_0 in the case II by changing the strength parameter q to study energy behavior of the elastic scattering amplitudes.

In both models, we limit ourselves by s-wave bound and continuum states in $\{12\}$ and projectile-target subsystems.

To construct the discrete representation of the $\{12\}$-continuum and to build the respective wave-packet states $|z_i\rangle$ we employ a diagonalization of the h_{12} Hamiltonian matrix on a finite Gaussian basis. It was demonstrated in our previous studies (see, e.g., Ref. [16]) that one can replace in practical calculations exact stationary wave-packets (i.e., those constructed using exact scattering states) with approximated packets in the form of discrete pseudostates of the Hamiltonian matrix found with some appropriate L_2 basis.

Thus, for the diagonalization of the sub-Hamiltonian h_{12} matrix the following Gaussian basis with many radial scales has been used:

$$\phi_n(r) = A_n \exp(-\alpha_n r^2), \quad n = 1, \ldots, N, \tag{24}$$

where A_n are the normalization coefficients and the "frequences" α_n are taken in the form of geometric progression [18]:

$$\alpha_n = \alpha_1 \left(\frac{\alpha_N}{\alpha_1}\right)^{\frac{n-1}{N-1}}, \quad n = 2, \ldots, N-1. \tag{25}$$

The key problem in the replacement of stationary wave-packets by the respective pseudostates is a correct evaluation of the normalization factors for the pseudostates or, alternatively, a correct determination of the pseudostate widths. Because these widths are tightly interrelated to the discretization bins, they, in essence, are just derivatives from the pseudostate energy distribution and can be found from the finite differences:

$$D_i = \begin{cases} \frac{[\epsilon_1^* + \epsilon_2^*]}{2}, & i = 1, \\ \frac{[\epsilon_{i+1}^* - \epsilon_{i-1}^*]}{2}, & i = 2, \ldots, N-1, \\ D_{N-1}, & i = N. \end{cases} \tag{26}$$

We have used in our calculations the basis set Eq. (24) with the scale parameters $\alpha_1 = 0.001$ fm^{-2}, $\alpha_N = 20$ fm^{-2} for two values of N: $N = 20$ and 40. In both cases, we have employed not all N pseudostates, but only those with eigenenergies less than 120 MeV. So, for both basis dimensions, the number of pseudostates N_{eff} used here are 12 and 20, correspondingly (including the bound state).

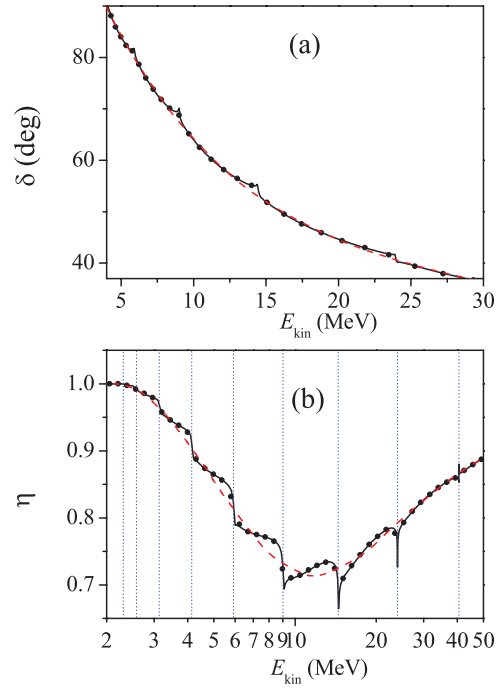

FIG. 1. (Color online) Partial phase shift δ (a) and inelasticity parameter $\eta = |S_{\text{el}}|$ (b) for the s-wave elastic scattering obtained within differential (full curve) and integral (dots) CCAs and also by full WP calculation (dashed curves) for model I. Vertical lines reflect the positions of pseudostates in the $\{12\}$ subsystem.

To discretize h_0 sub-Hamiltonian spectrum, the exact free wave-packet basis $\{|x_j\rangle\}$ [Eq. (15)] of the dimension M with bin endpoint distributed on the Chebyshev grid [19] have been employed:

$$\varepsilon_j = E_0 \tan\left(\frac{(2j-1)}{2M}\frac{\pi}{2}\right), \quad j = 1, \ldots, M. \tag{27}$$

The common energy scale parameter E_0 and the basis dimension M are chosen separately for each potential model.

B. Results for model I

The three-body elastic s-wave partial phase shifts and inelasticity parameters $\eta = |S_{\text{el}}|$ found via differential and integral CCAs and also by using the full WP calculation are represented in the Fig. 1.

It is clearly seen that partial phase shifts found within the both CCA approaches have the same singularities near the pseudostate energy thresholds. So, this singular energy behavior of the elastic amplitudes is caused directly by the coupled-channel approximation rather than the possible instabilities in numerical calculations. It should be stressed that the full three-body WP calculation leads to a rather smooth energy behavior of solutions.

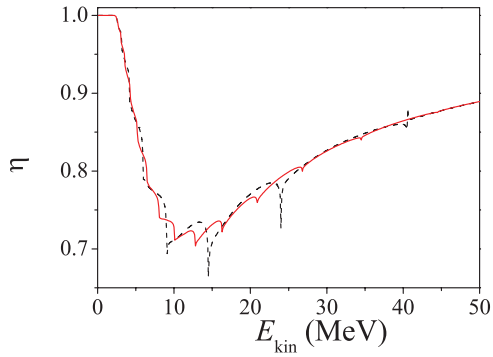

FIG. 2. (Color online) Inelasticity parameter for the s-wave elastic scattering amplitude η obtained within the differential CCA approach for model I for two basis sets of pseudostate with $N_{\text{eff}} = 12$ (dashed curve) and $N_{\text{eff}} = 20$ (solid curve).

Simultaneously, we observed that these irregularities do not vanish but become more narrow when the pseudostate basis dimension is increasing (see Fig. 2).

C. Results for model II

In this case, there are bound states in the fragment-target subsystems (for the real part of fragment-target interactions), and the full three-body system must include the rearrangement channels. Thus, the single LSE has a unique solution only if one includes the imaginary parts to the fragment-target interaction potentials. The bound states are shifted to the complex energy plane in that case.

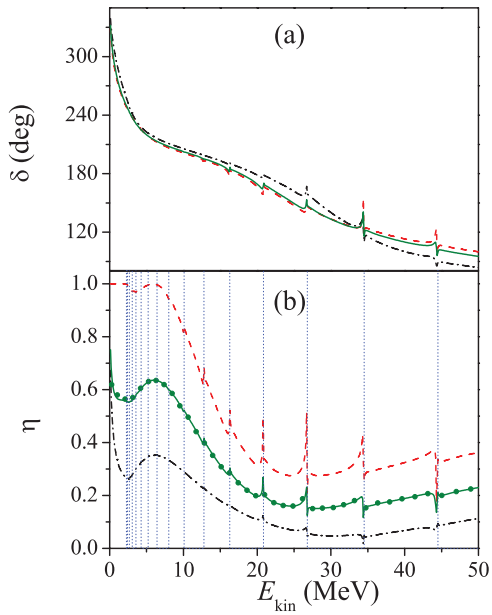

FIG. 3. (Color online) Partial phase shifts δ (a) and inelasticity parameters η (b) for the s-wave elastic scattering in model II obtained within the differential CCA approach for three different imaginary part parameter q of potential Eq. (23): $q = 0$ (dashed curves), $q = 0.1$ (solid curves), and $q = 0.25$ (dash-dotted curves). The filled circles on the solid curve in the Fig. 3(b) show the integral CCA results, while the vertical solid lines show pseudo-threshold positions.

In Fig. 3, the inelasticity parameters for potential Eq. (23b) with three values of imaginary part parameters: $q = 0$, 0.1, and 0.25 are represented. It is seen that the general energy behavior of the CCA results does not change significantly with increasing the coupling potential depths.

Also, it becomes clear that the energy irregularities near the pseudo-thresholds become more narrow and less visible when the imaginary parts of the coupling potentials get stronger. It will be shown below that these irregularities are nearly invisible for realistic optical fragment-target potentials and do not affect the energy behavior of the elastic scattering cross sections.

V. STUDY OF THE TEST CASE: $d + {}^{16}O$ ELASTIC SCATTERING

For the comprehensive comparison with the CCA scheme, we employed here some more realistic three-body model, viz. the elastic scattering of deuterons by the ^{16}O target using energy-independent nucleon-^{16}O optical potentials as input ones and keeping only s-wave NN interaction. Such a restriction does not effect to our main results and conclusions derived because our prime interest here is the accuracy of the CCA scheme in three-body scattering and the energy behavior of the elastic scattering amplitude. As interaction potentials in $N + {}^{16}O$ subsystems, we will use the respective nucleon-nucleus optical potentials (with parameter values taken from Ref. [3]).[3] In the present study, we consider the energy behavior of the three-body amplitudes in the energy range $E_{\text{c.m.}} = 5 \div 40$ MeV. Also, we will take into account the Coulomb interaction between deuteron center of mass and target nucleus.

The np interaction in deuteron channel is taken in the same form of a Gaussian potential Eq. (22) with the same parameters as in the previous section.

To construct the $\{np\}$ subsystem pseudostates, we use the same Gaussian basis Eq. (24) with scale parameters α_n distributed on the Chebyshev grid of the same type as Eq. (27) with the common scale parameter α_0. Our calculations have been carried out at $N = 15$ ($N_{\text{eff}} = 11$), $t = 1$, and $\alpha_0 = 0.1$.

In the $\{np\}$ subsystem, we limit ourselves only by s-wave bound and scattering states, while along the deuteron center-of-mass coordinate all angular momenta at $L \leqslant 30$ will be treated.

To discretize h_0 sub-Hamiltonian spectrum (which includes the long-range projectile-target Coulomb interaction in this case), we have used the Coulomb wave-packets [13] constructed numerically from the regular Coulomb wave-functions [similarly to the free wave-packet basis (15)] with bin endpoint distributed on the Chebyshev grid Eq. (27) with the dimension $M = 150$ and $E_0 = 20$ MeV.

The energy behavior of elastic amplitudes near the inelastic thresholds, as our study has demonstrated, *does depend* essentially upon the strength of imaginary part of nucleon-nucleus potential. Thus, to study this effect in detail we introduce some extra factor u upon which the imaginary parts of potentials $\text{Im}V_{n(p)A}$ are multiplied in three-body calculations.

[3]We take this optical potential at energy $E_N = 5.25$ MeV.

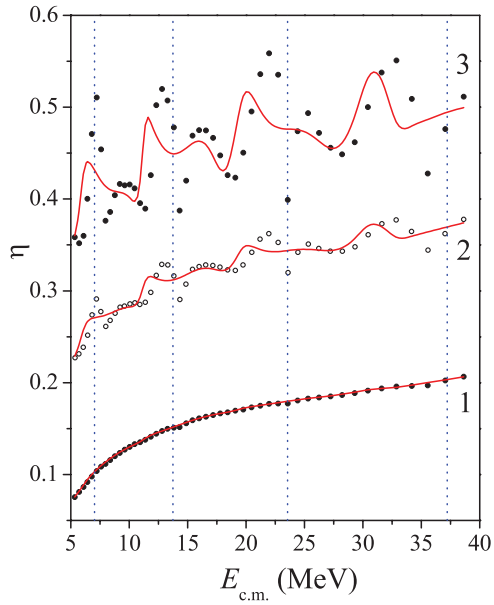

FIG. 4. (Color online) Inelasticity parameter η for the s-wave elastic $d + {}^{16}O$ scattering amplitude obtained within the full WP approach (solid curves) and PC approximation (circles) for different strengths of imaginary parts of the nucleon-nucleus interaction with factors: $u = 1.0$ (1), $u = 0.5$ (2), $u = 0.25$ (3). Vertical dotted lines define the positions of pseudostates in the $\{np\}$ subsystem.

The inelasticity parameter $\eta = |S_{el}|$ found from the elastic s-wave S matrix obtained in the full WP approach and within the PC approximation are presented in Fig. 4 for three values of the extra-factor $u = 1$ (the initial nucleon-nucleus potentials), 0.5, and 0.25. From the figure it is quite clear that the false near-threshold singularities in scattering amplitudes at $u = 1$ are invisible, while they are seen clearly at smaller values $u = 0.5$ and 0.25. These singularities are interrelated directly to the pseudostate energies. However, in the full WP calculation (i.e., that without CCA reduction) these singularities are smoothed out noticeably (see Fig. 4).

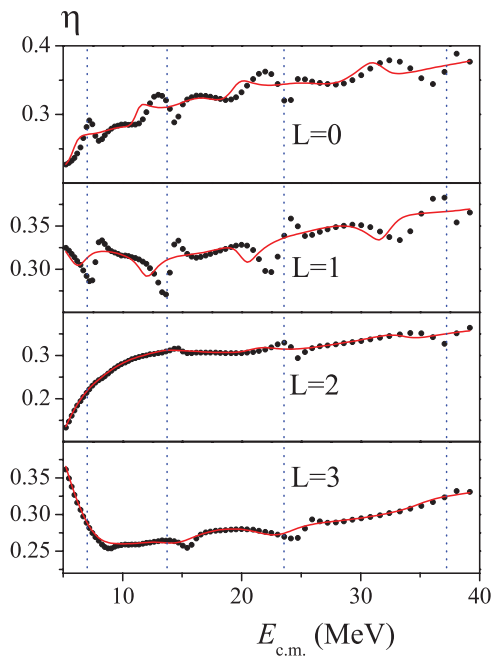

FIG. 5. (Color online) Inelasticity parameter η for the partial elastic $d + {}^{16}O$ scattering amplitudes obtained within the full WP approach (solid curves) and PC approximation (circles) for optical nucleon-target potential with half-strength imaginary parts (i.e., with $u = 0.5$) at different values of the total angular momentum L.

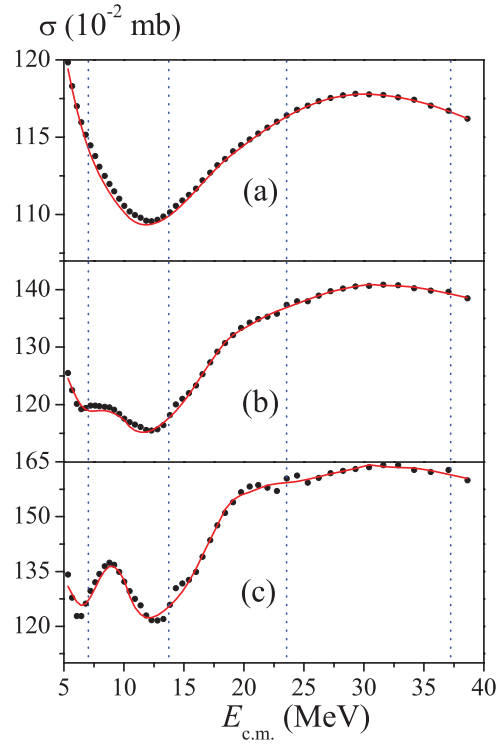

FIG. 6. (Color online) Elastic $d + {}^{16}O$ cross section obtained in the full WP approach (solid curves) and in the PC approximation (circles) for optical nucleon-target potentials with different extra-factors u: 1 (a), 0.5 (b), and 0.25 (c).

Then we study the higher partial amplitudes. The inelasticity parameter η_L at various angular momenta L are displayed in Fig. 5 for the half-strength imaginary part of nucleon-nucleus potentials. Our study has shown that the amplitude oscillations are seen only at lower partial waves, while at $L > 4$ these near-threshold irregularities are practically absent. This means that such irregularities in energy should be of no importance in the total cross-section behavior.

The cross-section energy dependence for the elastic scattering found with usage of the full WP calculation and PC approximation for three variants of the imaginary parts of the potentials is presented in Fig. 6. In this calculation, we have used the following formula for the elastic cross section:[4]

$$\sigma_{el} = \frac{\pi}{P^2} \sum_{L=0}^{L_{max}} (2L+1) \left| 1 - S_{el}^{L} \right|^2, \tag{28}$$

[4]We do not take into account the Coulomb part of the cross section here, only the nuclear part.

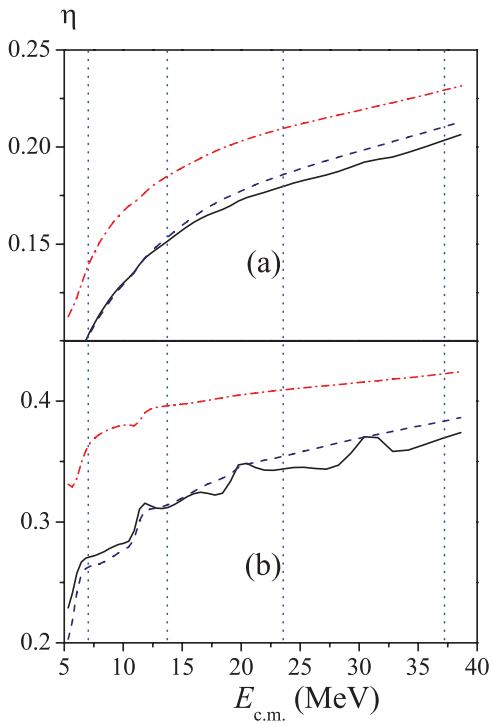

FIG. 7. (Color online) Inelasticity parameter η for s-wave elastic $d + {}^{16}O$ scattering amplitudes obtained within the full WP approach: the convergence over maximal excitation energy in the $\{np\}$ subsystem $E_{\max}$ for the full-strength (a) and half-strength imaginary parts (b) of the optical nucleon-nucleus potentials: $E_{\max} = 15$ MeV (dash-dotted curve), $E_{\max} = 25$ MeV (dashed curve), the full set of pseudostates (solid curve).

where P is the total momentum of the projectile and we employed the wave-packet approximation Eq. (20) for the elastic S-matrix element $S^L_{\rm el}$.

As is seen in Fig. 6, the PC approximation (i.e., CCA) leads to some distortion of the cross-section energy behavior only for the four-times reduced imaginary parts of the optical potentials. However, in such a case our full WP calculation gives a rather smooth result without any irregularities.

To complete the study, we considered a contribution and the effect of closed channels in the $\{np\}$ subsystem to the energy dependence of the elastic scattering amplitudes. For this study, we used three sets of s-wave pseudostates: (i) all the discrete pseudostates with energies $\epsilon^*_i \leqslant E_{\max} = 15$ MeV, (ii) all the pseudostates up to $E_{\max} = 25$ MeV, and (iii) the whole set of the pseudostates up to $E_{\max} = 100$ MeV.

For all three variants we calculated the inelasticity parameter η for the s-wave elastic amplitude found with the complete WPCD approach for two complex optical potentials with full-strength and half-strength imaginary parts; see Fig. 7. It follows from the results presented here that if the $E_{\max}$ value used is rather low and not sufficient to achieve the full convergence of the results, one has a wrong energy dependence for the scattering amplitudes (although rather smooth) even at the energies much less than $E_{\max}$. It confirms the well-known fact that the closed channel contribution is quite important at low collision energies.

VI. CONCLUSION

In this work we have examined the effects of the coupled-channel reduction in three-body scattering. We have demonstrated that the employment of the CCA when the two-body continuum is discretized with the conventional pseudostates leads to an appearance of irregularities in the three-body elastic scattering amplitudes near the pseudostate energies at lower total angular momenta. Such irregular behavior is better expressed at small imaginary parts of the nucleon-nucleus optical potentials. Nevertheless, the employment of the complete WPCD-technique (which is based on the full three-body continuum discretization) makes it possible to smooth false threshold effects. Also, we have shown that accurate account of close channel contributions is highly important at small and intermediate collision energies.

However, at energies $E_{\rm inc} \geqslant 20$ MeV typical for nuclear physics and when the low-L partial amplitudes are strongly suppressed by absorption effects, the CCA, e.g., in the form of the CDCC approach [5] is fully valid and reproduces the accurate results for *the restricted* (neglecting the rearrangement channels) three-body scattering problem. Moreover, we found that all the irregularities are smoothed strongly by increasing the imaginary part of the nucleon-nucleus interaction. Thus, our study seems to give the positive answer to the problem posed in long-term theoretical discussions about the general validity of the CCA and CDCC approaches in three- and few-body scattering problems (see, e.g., Ref. [12]).

ACKNOWLEDGMENTS

The authors appreciate partial financial support from the RFBR (Grant Nos. 10-02-00603 and 10-02-00096).

[1] S. Geltman and P. G. Burke, J. Phys. B **3**, 1062 (1970).
[2] I. Bray and A. T. Stelbovics, Phys. Rev. A **46**, 6995 (1992).
[3] M. Kawai, M. Kamimura, and K. Takesako, Progr. Theor. Phys. Suppl. **89**, 118 (1986).
[4] V. I. Kukulin and V. N. Pomerantsev, Yad. Fiz. (Sov. J. Nucl. Phys.) **50**, 27 (1989).
[5] R. A. D. Piyadasa, M. Kawai, M. Kamimura, and M. Yahiro, Phys. Rev. C **60**, 044611 (1999).
[6] R. Y. Rasoanaivo and G. H. Rawitscher, Phys. Rev. C **39**, 1709 (1989).
[7] I. J. Thompson, in *Scattering*, edited by E. R. Pike and P. C. Sabatier (Academic Press, New York, 2001), p.1360.
[8] J. R. Winick and W. P. Reinhardt, Phys. Rev. A **18**, 925 (1978).
[9] R. Kozack and F. S. Levin, Phys. Rev. C **36**, 883 (1987).
[10] Y. Suzuki, D. Baye, and A. Kievsky, Nucl. Phys. A **838**, 20 (2010).
[11] V. P. Popov and V. N. Pomerantsev, Phys. Rev. A **83**, 032516 (2011).
[12] T. Sawada and K. Thushima, Prog. Theor. Phys. **76**, 440 (1986).

[13] O. A. Rubtsova, V. I. Kukulin, and A. M. Moro, Phys. Rev. C **78**, 034603 (2008).
[14] O. A. Rubtsova, V. N. Pomerantsev, and V. I. Kukulin, Phys. Rev. C **79**, 064602 (2009).
[15] V. N. Pomerantsev, V. I. Kukulin, and O. A. Rubtsova, Phys. Rev. C **79**, 034001 (2009).
[16] V. I. Kukulin *et al*., Theor. Math. Phys. **150**, 403 (2007).
[17] A. Messiah, *Quantum Mechanics* (North-Holland, Amsterdam, 1965).
[18] E. Hiyama, Y. Kino, and M. Kamimura, Progr. Part. Nucl. Phys. **51**, 223 (2003).
[19] V. I. Kukulin *et al*., Nucl. Phys. A **453**, 365 (1986).